Anticancer Activity of the Antibiotic Clioquinol

Wei-Qun Ding, Bolin Liu, Joshua L. Vaught, Hanako Yamauchi, and Stuart E. Lind

Departments of Pathology and Medicine, University of Oklahoma Health Sciences Center, Oklahoma City, Oklahoma

Abstract

Clioquinol, a metal chelator, has been used for many years as an antimicrobial agent and more recently as a potential treatment for Alzheimer's disease. Because it binds copper and zinc, metals essential for the activity of the enzyme superoxide dismutase-1 (SOD1), a potential target for anticancer drug development, we investigated its effects on human cancer cells. Treatment with clioquinol reduced the viability of eight different human cancer cell lines in a concentration-dependent manner, with IC_{50} values in the low micromolar range. Biochemical analysis revealed that clioquinol induced cancer cell death through apoptotic pathways that require caspase activity. Although clioquinol induced modest inhibition of SOD1 activity in treated cells, comparable inhibition by a known SOD1 inhibitor, diethyldithiocarbamate, did not result in cytotoxicity. The addition of copper, iron, or zinc did not rescue cells from cliquinol-induced cytotoxicity but enhanced its killing, arguing against metal chelation as its major mechanism of action. To test if clioquinol might act as an ionophore, a fluorescent probe was used to monitor intracellular zinc concentrations. The addition of clioquinol resulted in elevated levels of intracellular zinc, indicating that clioquinol acts as a zinc ionophore. In an *in vivo* xenografts mouse model, clioquinol inhibited tumor growth of xenografts over a 6-week period, without inducing visible toxicity. Our results show that clioquinol has anticancer effects both *in vitro* and *in vivo*. Transition metal ionophores may be a subclass of metal chelators with anticancer activity deserving of further development. (Cancer Res 2005; 65(8): 3389-95)

Introduction

It has been known for some time that metals (such as copper and iron) are involved in the development of cancer and have been shown to be important for both carcinogenesis (1–3) and angiogenesis (4). Metal chelators such as desferrioxamine, an iron chelator (5), and tetrathiomolybdate, a copper chelator (6), have been shown to suppress tumor growth, metastases, and angiogenesis and are currently being investigated in clinical trials (5, 7, 8). Chelation of metals may have antitumor effects via several different intracellular mechanisms. Iron chelators, for example, have been shown to induce apoptosis through a p53-independent pathway (9) and by the inhibition of N-*myc* expression (10), whereas copper chelators induce apoptosis of tumor cells through the inhibition of the NFκB signaling cascade (11).

Clioquinol (5-chloro-7-iodo-8-hydroxyquinoline) is a chelator of copper, zinc, and iron. It was first prepared in Germany in the early part of the last century (12) and was widely used as an antibiotic for the treatment of diarrhea and skin infection. In the 1970s, it was linked to an outbreak of subacute myelo-optic neuropathy in Japan (13) and was banned in many countries. Subsequent epidemiologic analysis questioned the link between subacute myelo-optic neuropathy and clioquinol (14) and it remains available in several countries, including Canada, where it is sold in a topical preparation. In 2001, the metal-binding properties of clioquinol led to its use in a mouse model of Alzheimer's disease in which it was shown to reduce or prevent the formation of amyloid plaques in the brain (15). It was also shown to have efficacy in an animal model of Parkinson's disease (16). Clioquinol was then moved into clinical trials for patients with Alzheimer's disease. It proved nontoxic in a small Swedish trial (17) involving 20 patients. A larger trial conducted in Australia involved 36 patients who received the drug orally in increasing doses over a 10-month period. The study, reported at the end of 2003, showed (1) no toxicity in any patients, (2) clinical benefit in some patients, and (3) trough steady-state blood levels of 25 μmol/L at the highest dose level (18).

Superoxide dismutase-1 (SOD1) is an important enzymatic defense against oxidative stress that has been shown to be a potentially useful target for anticancer therapy (19). Because SOD1 uses both copper and zinc as cofactors, we postulated that clioquinol might have antitumor activity by virtue of chelating one or both of these metals. As reported here, we found that clioquinol exhibits antitumor activity *in vitro* and *in vivo*, but does not seem to do so because of SOD1 inhibition or simple metal chelation. Instead, our studies suggest the mechanism of action of clioquinol is due to its ability to act as a transition metal ionophore, a class of compounds not previously considered as potential anticancer agents.

Materials and Methods

Materials. The CellTiter 96 Aqueous ONE Solution (Promega, Madison, WI) was used to assess cellular viability via reduction of 3-(4,5-dimethylthiazol-2-yl)-5-(3-carboxymethoxyphenyl)-2-(4-sulfophenyl)-2*H*-tetrazolium (MTS). Nude mice were from Harlan Sprague-Dawley Inc. (Indianapolis, IN). All other reagents were analytic grade and obtained from Sigma Chemical Co. (St. Louis, MO), unless otherwise stated.

Cell culture and viability assay. DHL-4 cells were provided by Dr. Linda Boxer (Stanford University), A2780 cells by Dr. Stephen Howell (University of California, San Diego), and SiHa cells by Dr. Doris Benbrook (University of Oklahoma). All other cells were obtained from the American Type Culture Collection (Manassas, VA). Cells were routinely grown in a 75-mm flask in an environment containing 5% CO_2 and passed every 3 days. Cell viability was analyzed using the MTS assay. Depending on growth properties of each cell line, 2,000 to 20,000 cells were plated in each well of a 96-well tissue culture plate with 100 μL of medium, which resulted in 40% to 50% confluence of the cells after 24 hours of growth. The medium was then replaced with 100 μL of fresh medium containing clioquinol or other reagents, and the cells were grown for designated periods. The MTS assay was done using the protocol provided by the manufacturer. In short, 20 μL of MTS solution was added to each well, and cells were incubated at 37°C for 1 to 2 hours. The absorbance (at 490 nm) of each well was then determined. Data are presented as a percentage of the values obtained from cells cultured under the same

Requests for reprints: Wei-Qun Ding, University of Oklahoma Health Sciences Center, 975 Northeast 10th Street, BRC-409, Oklahoma City, OK 73104. Phone: 405-271-1605; Fax: 405-271-6289; E-mail: weiqun-ding@ouhsc.edu.

conditions in the absence of clioquinol or other chemicals. For the time course study of clioquinol cytotoxicity, A2780 cells were treated with 30 μmol/L clioquinol for different times. At different time points, the medium containing clioquinol was removed by aspiration. Cells were washed twice and fresh medium without clioquinol was added. Cell viability was analyzed 72 hours after the initiation of clioquinol treatment, using the MTS assay.

Western blot analysis. Western blot analysis was done as previously described (20–22). Briefly, cells were lysed in a lysis buffer containing 50 mmol/L Tris (pH 7.4), 50 mmol/L NaCl, 0.5% NP40, 50 mmol/L NaF, 1 mmol/L Na_3VO_4, 1 mmol/L phenylmethylsulfonyl fluoride, 25 μg/mL leupeptin, and 25 μg/mL aprotinin. The lysates were centrifuged at 15,000 × *g* for 15 minutes and the supernatants were collected for protein concentration determination, SDS-PAGE, and Western blot analysis with specific antibodies, as described in the figure legends.

Quantification of apoptosis by ELISA. An ELISA-based kit (Roche Diagnostics Corp., Indianapolis, IN) was used to quantitatively measure cytoplasmic histone–associated DNA fragments (mononucleosomes and oligonucleosomes), a measure of apoptosis, according to the manufacturer's instructions.

Caspase-3 activity assay. The enzymatic activities of caspase-3 were measured by using a colorimetric assay kit (Clontech Laboratories Inc., Palo Alto, CA). The assay is based on spectrophotometric detection of the chromophore *p*-nitroanilide, which is cleaved from the specific substrate Ac-DEVD-chromophore *p*-nitroanilide (Alexis Corp., San Diego, CA) by activated caspase-3.

Xenograft model. Nude mice were maintained in accordance with the Institutional Animal Care and Use Committee procedures and guidelines. A total of 10×10^6 Raji (a human B-cell lymphoma line) or 5×10^6 A2780 (a human ovarian cancer line) cells were suspended in 100 μL of PBS, mixed with 50% Matrigel, and injected s.c. into the flanks of 5-week-old female nude mice. Clioquinol was dissolved in Intralipid 20% (Fresenius Kabi Clayton, L.P., Clayton, NC), a soy-based lipid emulsion used to provide parenteral nutrition to human subjects. Control animals were given an identical volume (1 mL) of the carrier emulsion without clioquinol. Animals were treated by i.p. injection at a clioquinol dose of 28 mg/kg, 5 days a week, beginning 8 days after tumor inoculation, until the time of death. Calipers were used to measure the greatest (length of tumor) and perpendicular (width of tumor) diameters three times a week. The tumor volume was calculated with the formula: $v = l \times w^2 \times 0.5$, where v is the tumor volume, l the length of tumor, and w the width of tumor (23). Animals' weights were also measured three times a week. In accordance with institutional animal committee guidelines, animals were killed when their tumor volume equaled 10% of their body mass (assuming a tumor volume of 1 mm^3 weighs 1 g). The survival curves were determined by the Kaplan-Meier method. The log-rank test was used to assess the differences in survival curves. Both analyses were done with a computer program (Graphpad Prism, Graphpad Software, San Diego, CA).

Table 1. IC_{50} values of clioquinol for the viability of human cancer cell lines

Cell line	Tumor type	IC_{50} (μmol/L)
DHL-4	B cell	6.7
Raji	B cell	12.4
A2780	Ovarian	14.2
MDA-MB-231	Breast	19.9
T24	Bladder	20
M-Panc-96	Pancreas	23.6
MCF-7	Breast	29.7
SiHa	Cervical	38.8
3T3	Fibroblast	43.1

NOTE: Cells were plated in 96-well plates and treated with 0.1, 1, 3, 10, 30, and 100 μmol/L of clioquinol for 72 hours. Cell viability was determined using the MTS assay. IC_{50} values were calculated by nonlinear regression analysis (n = 3). The mouse 3T3 fibroblast cell line was included in the study.

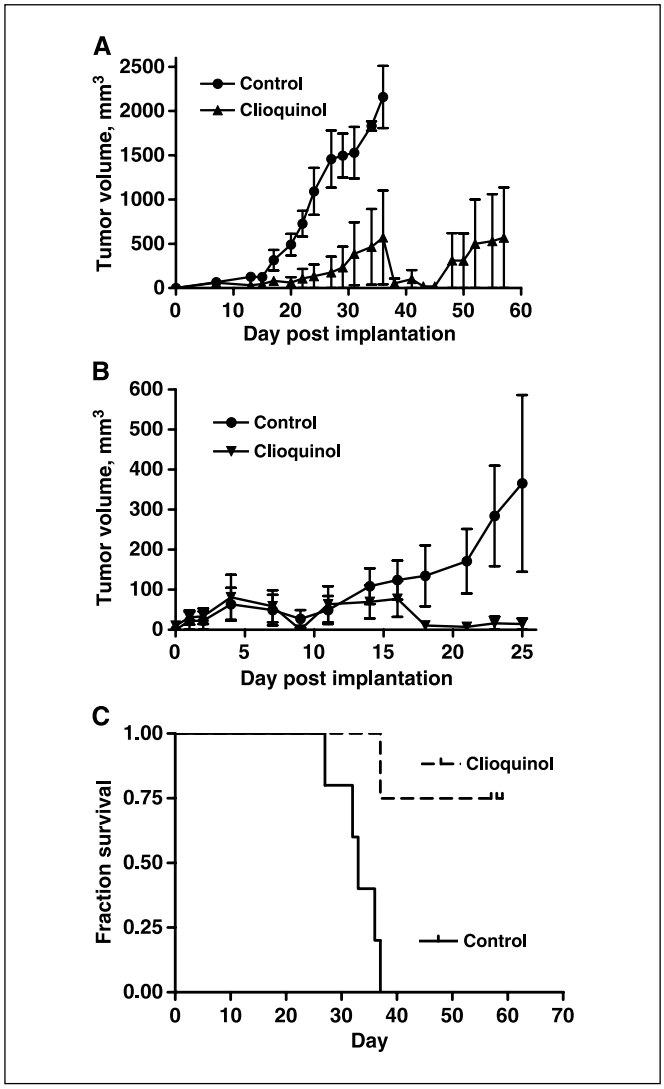

Figure 1. Effects of clioquinol on tumor growth in nude mice. Raji and A2780 cells were injected s.c. into the flanks of 5-week-old female nude mice. Clioquinol (28 mg/kg) was given i.p. 5 days a week, starting on day 8 after implanting. Tumor volume was calculated and expressed as cubic millimeters (mean ± SE; control group, n = 4; clioquinol group, n = 5). *A,* inhibition of tumor growth of A2780 cells in nude mice. *B,* inhibition of tumor growth of Raji cells in nude mice. *C,* survival curve of A2780 cell–implanted mice.

Superoxide dismutase-1 activity analysis. SOD1 activity was assayed using the xanthine oxidase/xanthine/cytochrome *C* method as previously described (24). Briefly, the control reaction was started by adding 1 unit of xanthine oxidase to a reaction mixture containing 15 μmol/L cytochrome *C*, 100 μmol/L xanthine in 50 mmol/L potassium phosphate, and 0.1 mmol/L EDTA (pH 7.8) at 25°C in a 96-well plate. The absorbance of the plate was read every 15 seconds for up to 20 minutes at 550 nm. SOD1 activity was assayed by adding one unit of purified bovine erythrocyte SOD1 or 15 μg of cellular extract to the control reaction mixture before the addition of xanthine oxidase. Cell extracts were prepared after 6 hours' treatment of Raji cells with 100 μmol/L of clioquinol or 1 mmol/L of diethyldithiocarbamate. Cells were pelleted, dissolved in PBS buffer, sonicated, and centrifuged to remove nuclei. Cytosolic protein concentrations were determined with a protein assay kit (Bio-Rad Laboratories, Hercules, CA).

Cellular zinc-level measurements. A sensitive water-soluble salt form of the high-affinity fluorescent zinc indicator Fluo-Zin-3 (Molecular Probes, Eugene, OR) was used. A2780 (10,000 cells per well) or Raji cells (30,000 cells per well) were plated in a 96-well plate. Twenty-four hours after plating, the cells were treated with 30 μmol/L clioquinol or 10 μmol/L pyrithione for 1 hour in the presence of various concentrations of zinc. FluoZinc-3 (3 μmol/L, final concentration) was added and the cells were incubated for another 30 minutes at 37°C. After the incubation, cells were washed twice with fresh medium to remove any dye nonspecifically associated with the cell surface. Additional medium was added and the cells were incubated for a further 30 minutes before fluorescence measurements were made. The fluorescence was measured at 485/535 nm (excitation/emission), using a Wallac 1420 Multilabel Counter (Perkin-Elmer Life Sciences, Boston, MA).

DNA transfection and NFκB activity assay. A well-established NFκB-luciferase plasmid construct (pNF-κB-Luc, BD Biosciences Clontech, Palo Alto, CA) was used for NFκB activity study. A2780 cells (0.8×10^6) were initially seeded in 100-mm dishes in 10 mL of RPMI 1640 with supplements. Twenty-four hours after plating, cells were washed with PBS and incubated with lipofectin-DNA complexes for 6 hours. Lipofectin-DNA complexes were made by incubating 25 μL of lipofectin reagent with 4 μg of plasmid DNA in 0.2 mL of serum-free RPMI 1640 for 40 minutes at 22°C. The medium was exchanged with RPMI 1640 with supplements after 5 hours of transfection and cells were incubated overnight. The cells then were plated into 24-well plates at a density of 100,000 per well.

After 48 hours of transfection, cells were treated with clioquinol at various concentrations for 4 hours or at 30 μmol/L for 1 hour in the presence of $ZnCl_2$. For luciferase activity assay, cells were washed once with PBS in the absence of Mg^{2+} and Ca^{2+} and lysed with 200 μL of reporter lysis buffer (Promega). The cell particulate was removed by brief centrifugation, and the protein concentration was measured. Luciferase assays were done using a Turner TD/20E luminometer with 30 μL of luciferase assay reagent mixed with 50 μL of protein extract. The relative light units were normalized for the amount of protein in each extract, and the results were reported as relative changes in luciferase activity.

Statistics. Differences among groups of data were assessed using one-way ANOVA followed by Dunnett or Bonferroni analysis with $P < 0.05$ as the level of statistical significance. All statistical analyses were done with Graphpad Prism software.

Results

Clioquinol induces cytotoxicity in human cancer cell lines. We first examined the effects of clioquinol on the viability of eight human cancer cell lines representing different tissues of origin. The cells studied included human B-cell lymphoma lines (DHL-4, Raji) and breast (MCF-7, MDA-MB231), ovarian (A2780), cervical (SiHa), bladder (T24), and pancreatic (Mpanc-96) cancer cells. The mouse 3T3 fibroblast cell line was also included. As shown in Table 1, treatment with clioquinol for 72 hours reduced viability of all cell

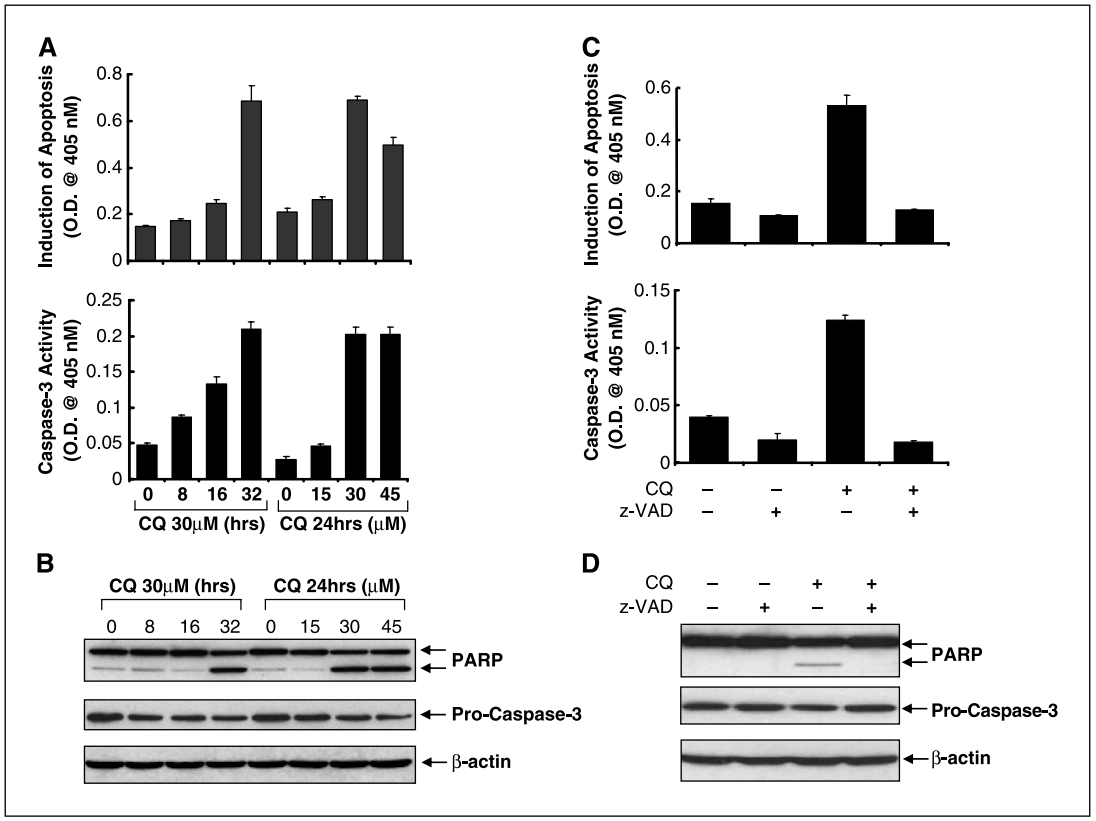

Figure 2. Clioquinol induces apoptosis in Raji cells through caspase-dependent mechanism. *A,* induction of apoptosis and caspase-3 activation by clioquinol (*CQ*). Raji cells were plated in 75-mm^2 flasks at 3×10^6 cells per flask and treated with 30 μmol/L clioquinol for indicated time points or 24 hours with clioquinol for indicated concentrations. Cell lysates were prepared and subjected to apoptosis ELISA (*top*) and caspase-3 activity assay (*bottom*). *B,* an equal amount of protein for each sample as prepared in (*A*) was resolved by 8% SDS-PAGE followed by Western blot analysis with specific antibodies directed against PARP (BIOMOL Research Laboratories Inc., Plymouth Meeting, PA), caspase-3 (clone 19, monoclonal antibody, Transduction Laboratories, Lexington, KY), or β-actin (Sigma). *C,* abrogation of clioquinol-induced apoptosis and caspase-3 activation by caspase-specific inhibitor. Raji cells were plated in 75-mm^2 flasks at 3×10^6 cells per flask and treated for 24 hours with either 30 μmol/L clioquinol or caspase pan-inhibitor z-VAD-fmk (Calbiochem Corp., San Diego, CA) alone or in combination of clioquinol and z-VAD-fmk. Cell lysates were prepared and subjected to apoptosis ELISA (*top*) and caspase-3 activity assay (*bottom*). *D,* an equal amount of protein for each sample as prepared in (*C*) was resolved by 8% SDS-PAGE, followed by Western blot analysis with specific antibodies directed against PARP, caspase-3, or β-actin. *A* and *C,* data (mean ± SE, $n = 3$) are expressed as actual readings. *B* and *D* are representative of three independent experiments.

lines tested, with IC_{50}s ranging from 10 to 40 μmol/L, concentrations that are similar to trough levels found in the blood of patients receiving p.o. clioquinol in a clinical trial for Alzheimer's disease (18). Time course studies indicated that exposure to 30 μmol/L clioquinol for 2 hours caused 25% reduction of cell viability, whereas exposure for 8 hours was sufficient for full cytotoxicity toward A2780 cells to be shown.

Clioquinol inhibits tumor growth in nude mice bearing human tumor cells. To determine whether clioquinol exhibits antineoplastic activity *in vivo,* xenografts of either Raji or A2780 cells were grown s.c. in the flanks of nude mice. Clioquinol was dissolved in Intralipid 20% (a Food and Drug Administration–approved soy-based emulsion used clinically in humans) and given by i.p. injection starting on day 8 after tumor cell inoculation for the duration of the experiment. The control group received an identical volume of the carrier emulsion alone on the same schedule. Toxicity was assessed by monitoring the animals for weight loss or for signs of altered motor or neurologic function while in their cages. No clioquinol-treated animals exhibited weight loss or clinical signs of toxicity during 6 weeks of treatment. Clioquinol-treated animals exhibited normal grooming behavior and gained weight during the 6-week treatment period. As shown in Fig. 1, administration of clioquinol in two separate experiments resulted in significant inhibition of growth of both Raji and A2780 xenografts. Although the Raji xenografts grew too slowly to result in shortening of the animals' survival (defined by the attainment of a tumor volume/weight equal to 10% of the animal's weight), A2780 xenografts grew rapidly in untreated mice. Clioquinol prolonged survival of treated animals bearing A2780 xenografts ($P = 0.01$; Fig. 1*C*).

Clioquinol induces apoptosis through caspase-dependent pathways. To determine whether clioquinol induced apoptosis, Raji cells were analyzed after treatment for 12 to 24 hours. Apoptosis was assayed by measuring the generation of cytoplasmic histone–associated DNA fragments. Figure 2*A* shows that clioquinol induces apoptosis in a time- and concentration-dependent manner. Western blot of cytosolic extracts prepared from clioquinol-treated cells revealed cleavage of the 116-kDa protein poly(ADP-ribose) polymerase (PARP) and generation of a 89-kDa fragment (Fig. 2*B*; refs. 20–22). The appearance of the 89-kDa PARP fragment coincided with the activation of caspase-3, as shown by the reduced level of the 32-kDa proenzyme and the caspase-3 activity assay (Fig. 2*A* and *B*). Furthermore, the clioquinol-induced apoptosis, PARP cleavage, and caspase-3 activity were abrogated by pretreatment of Raji cells with the caspase pan-inhibitor z-VAD-fmk (80 μmol/L) for 1 hour (Fig. 2*C* and *D*). These results indicate that clioquinol induces apoptosis that requires caspase activity.

Possible mechanisms of clioquinol-mediated cytotoxicity. Our initial hypothesis was that clioquinol would be cytotoxic toward tumor cells by virtue of chelating zinc and/or copper, thereby inactivating SOD1. To test this hypothesis, we analyzed the effect of clioquinol on the activity of purified SOD1 on superoxide generated by xanthine and xanthine oxidase (24). As shown in Fig. 3, clioquinol inhibited the enzymatic activity of purified bovine erythrocyte SOD1 in a concentration-dependent manner and had a modest effect on the SOD1 activity of cytosolic extracts prepared from clioquinol-treated Raji cells. However, treatment of cells with diethyldithiocarbamate, a known SOD1 inhibitor (25), at concentrations up to 1 mmol/L, caused a similar reduction in SOD1 activity without inducing cytotoxicity (data not shown). This suggested that clioquinol cytotoxicity toward tumor cells was not due to its attenuation of SOD1 activity.

To test whether clioquinol cytotoxicity was related to its chelating ability, we added zinc, copper, or iron to clioquinol-treated Raji cells to determine whether supplementation would block cell killing. Rather than rescuing the cells, as would be expected if a chelated metal was repleted, each of the metals enhanced clioquinol cytotoxicity in a concentration-dependent manner (Fig. 4). This finding argues against metal chelation as a major mode of action. Additional combinations of these metals at lower concentrations also increased, rather than decreased, clioquinol-mediated cytotoxicity (data not shown).

Because clioquinol is a metal-binding compound, the failure of metal supplementation to rescue the cells raised the possibility that clioquinol might be cytotoxic because it binds metals extracellularly and transports them into the cells. Iron and copper are redox-active metals, which may be more redox active when complexed with some chelators, and are well recognized to be cytotoxic. Zinc, on the other hand, is not a redox-active metal (26) and has been reported to inhibit apoptosis under certain circumstances (27, 28). We therefore focused on the effects of treating cells with clioquinol and zinc. [Recent work has shown that zinc may be cytotoxic for certain cell types, including neurons (29), thymocytes (30), and leukemia cells (31)]. For comparison, we used pyrithione, a known zinc ionophore. As shown in Fig. 5*A*, zinc potentiated both clioquinol- and pyrithione-induced cytotoxicity toward Raji cells in a concentration-dependent manner. Treatment of Raji cells with

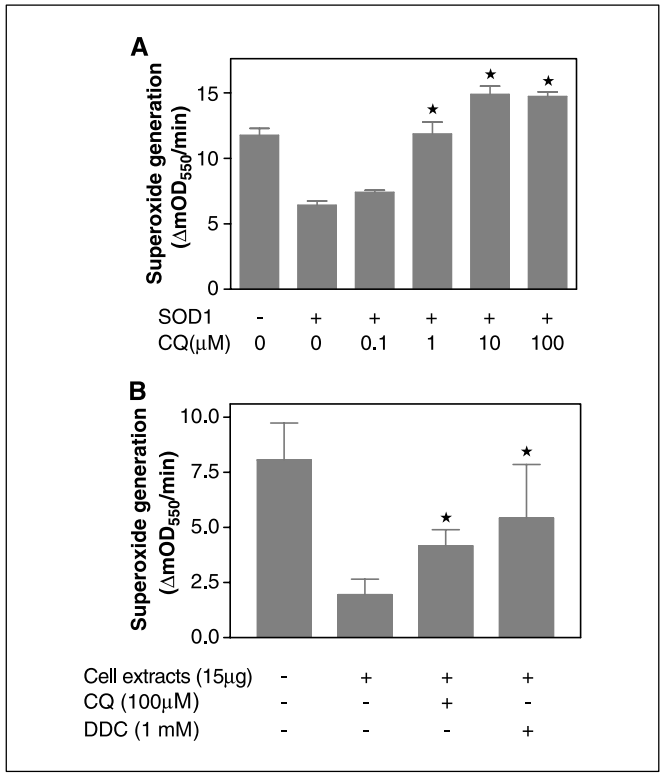

Figure 3. Effects of clioquinol on SOD1 activity. SOD1 activity was assayed with the xanthine oxidase/cytochrome *C* method as described in Materials and Methods. One unit of purified bovine erythrocyte SOD1 and 15 μg cellular extracts were used for the assay. *A,* clioquinol inhibits SOD1 activity in a concentration-dependent manner. *B,* clioquinol (100 μmol/L) and diethyldithiocarbamate (*DDC*, 1 mmol/L) inhibit SOD1 activity in Raji cells after 6 hours' treatment. Data (mean ± SE) are obtained from four to six independent experiments. *, $P < 0.05$, compared with SOD1 activity control (*second bar*), using one-way ANOVA followed by Bonferroni analysis.

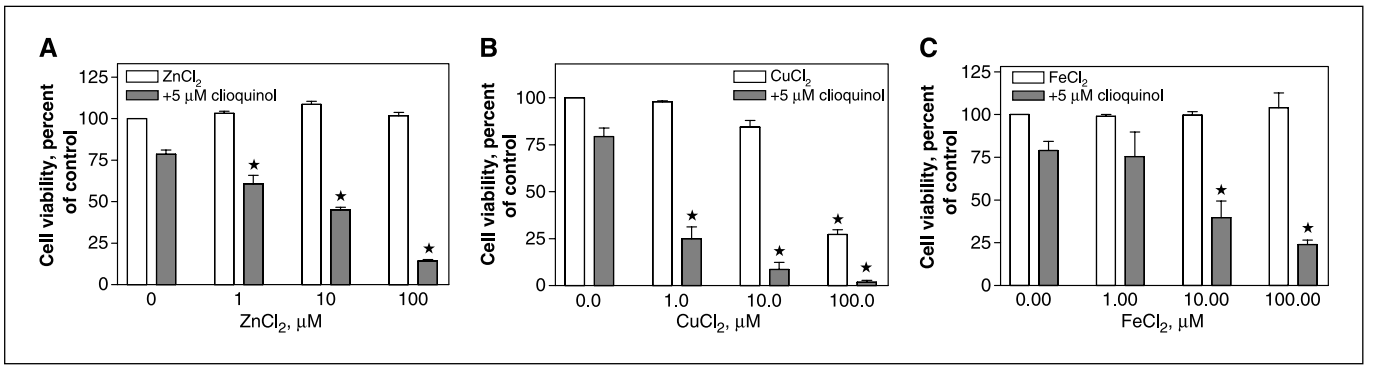

Figure 4. Addition of metals enhances clioquinol cytotoxicity in Raji cells. Cells were treated with $ZnCl_2$, $CuCl_2$, and $FeCl_2$ alone or premixed with 5 μmol/L clioquinol. After 72 hours of incubation, cell viability was determined using the MTS assay. Data (mean ± SE, $n = 3$) are expressed as a percentage of untreated control cells. *, $P < 0.05$, compared with control cells, using one-way ANOVA followed by Dunnett analysis.

N,*N*,*N*′,*N*′-tetrakis (2-pyridyl-methyl)ethylenediamine (TPEN), a cell-permeable, high-affinity zinc chelator (32), had moderate cytotoxic effects, which was rescued by 100 μmol/L zinc (Fig. 5*B*), further arguing against chelation as a mechanism of clioquinol cytotoxicity.

To determine directly whether clioquinol is able to serve as an ionophore, experiments were done using a fluorescent zinc-binding probe. Significant increases in fluorescence were detected in both A2780 and Raji cells that had been treated with 30 μmol/L clioquinol or 10 μmol/L pyrithione in the presence of various concentrations of zinc, as shown in Fig. 6. These experiments confirm that clioquinol acts as a zinc ionophore in these cells.

Because zinc has been reported to be involved in the down-regulation of NFκB activity by pyrithione (33) and pyrrolidine dithiocarbamate (34), we tested the effects of clioquinol on NFκB activity using a well-established NFκB-luciferase reporter gene construct. Treatment of A2780 cells with clioquinol for 4 hours caused an attenuation of NFκB activity in a concentration-dependent manner (Fig. 6*C*). When zinc was added together with 30 μmol/L clioquinol to the cells, NFκB activity was dramatically diminished and these striking inhibitory effects were detected at 1 hour of treatment and dependent on zinc concentrations. Pyrrolidine dithiocarbamate (30 μmol/L) plus zinc (100 μmol/L) served as positive control (Fig. 6*D*). When 10 μmol/L TPEN and 100 μmol/L zinc were applied to the cells, NFκB activity was slightly enhanced (data not shown). Because NFκB signaling has been known to be constitutively activated in tumor cells and is considered as a valid molecular target for chemotherapy (35), these results suggest that zinc ionophores may be a group of compounds that can be developed into chemotherapeutic agents.

Discussion

The present study shows that the antibiotic clioquinol has anticancer properties, as shown by both *in vitro* and *in vivo* experiments. Clioquinol has a long history of human use but has not been previously studied as an anticancer agent. Although it has been implicated in the causation of subacute myelo-optic neuropathy in Japan, experimental evidence suggests that decreased levels of vitamin B_{12} may play a role in this syndrome (36) and that clioquinol may be used safely in humans with vitamin B_{12} supplementation (17). More importantly, the IC_{50} values on tumor cell viability for clioquinol are not dissimilar from the trough blood concentrations documented in a recent clinical trial of clioquinol in patients with Alzheimer's disease (18). The apparent tolerability of normal tissues for clioquinol in the face of tumor growth inhibition seen in xenograft-bearing animals may relate to the fact that clioquinol binds albumin with high affinity (37) and albumin selectively targets tumors (38).

Several metal chelators have been shown to have antitumor effects and are currently being investigated in clinical trials (5, 7, 8). Although the studies reported here were initiated because we thought clioquinol might prove to be another useful chelator, the results suggest that the antitumor activity of clioquinol is not due to its ability to chelate metals. Whereas supplementation with the key

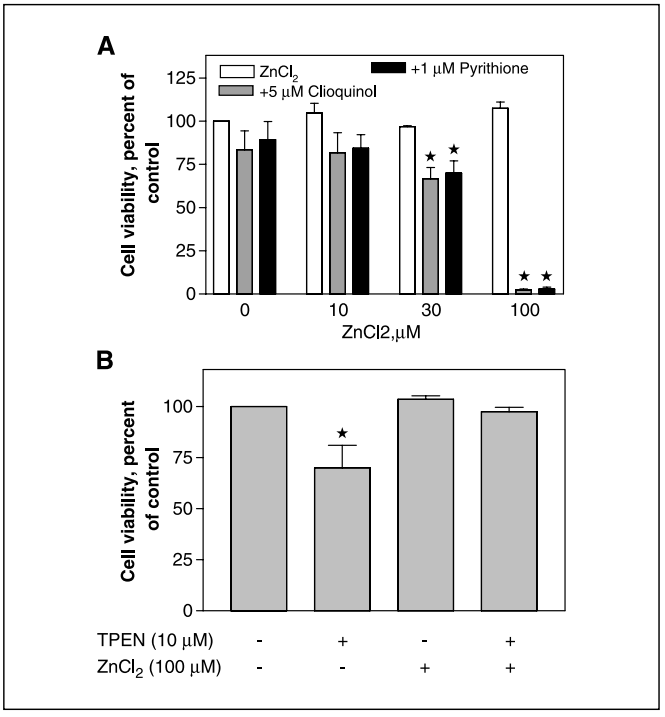

Figure 5. Effects of zinc-binding compounds on the viability of Raji cells. *A,* cells were grown in RPMI 1640 with supplements and treated with 5 μmol/L clioquinol or 1 μmol/L pyrithione for 72 hours in the presence of 10, 30, or 100 μmol/L $ZnCl_2$. *B,* cells were treated with 10 μmol/L TPEN and 100 μmol/L $ZnCl_2$ for 72 hours. Cell viability was analyzed with the MTS assay. Data (mean ± SE, $n = 3$) are expressed as a percentage of untreated control cells. *, $P < 0.05$, compared with control cells, using one-way ANOVA followed by Dunnett analysis.

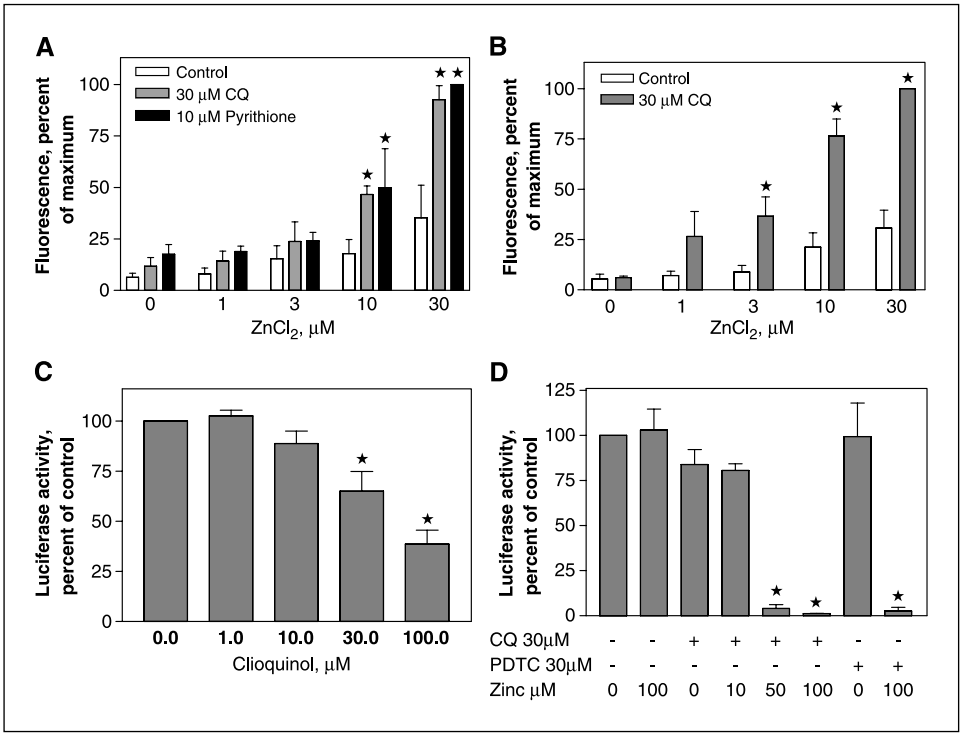

Figure 6. Effects of clioquinol on zinc uptake and NFκB activity. *A,* A2780 cells were treated with 30 μmol/L clioquinol and 10 μmol/L pyrithione for 1 hour in the presence of various $ZnCl_2$ concentrations. *B,* Raji cells were treated with 30 μmol/L clioquinol for 1 hour in the presence of various $ZnCl_2$ concentrations. The FluoZin-3 probe (3 μmol/L) was then added to A2780 or Raji cells. After 30 minutes of incubation, cells were washed with fresh RPMI 1640 twice and kept in the incubator for another 30 minutes. The fluorescence was recorded at 485/535 nm (excitation/emission), using a Wallac 1420 Multilabel Counter. *A* and *B,* data (mean ± SE, $n = 3$) are expressed as a percentage of maximum fluorescence detected. *C,* A2780 cells were treated with clioquinol for 4 hours at indicated concentrations. *D,* A2780 cells were treated with 30 μmol/L clioquinol for 1 hour in the presence of various $ZnCl_2$ concentrations or with 30 μmol/L pyrrolidine dithiocarbamate (*PDTC*) for 1 hour in the presence of 100 μmol/L $ZnCl_2$. Cell lysates were prepared and luciferase activity assayed as described in Materials and Methods. *C* and *D,* data (mean ± SE, $n = 3$) are expressed as percentages of untreated control cells. *, $P < 0.05$, compared with control cells, using one-way ANOVA followed by Dunnett analysis.

metal(s) bound by a chelator would be expected to overcome the cytotoxic effects of a chelator, we found that addition of copper, iron, and/or zinc did not overcome clioquinol-induced cytotoxicity, but in fact enhanced it. In addition, the high-affinity zinc chelator TPEN ($K_d = 10^{-15}$; ref. 32) did not have the same cytotoxic effect as clioquinol, which has a lower affinity for zinc ($K_d = 10^{-7}$; ref. 15). Suspecting that clioquinol was acting as an ionophore, we used a fluorescent zinc probe to show that clioquinol, like pyrithione ($K_d = 10^{-6}$; ref. 32), increased intracellular zinc concentrations. Moreover, clioquinol, like other zinc ionophores, down-regulates NFκB signaling. Taken together, these results suggest that clioquinol has antineoplastic activity not simply because it binds metals but because it can transport them intracellularly.

A previous study examining the mechanism of clioquinol neurotoxicity used neural crest–derived melanoma cells and reported that 24 hours' exposure to a clioquinol-zinc chelate was cytotoxic and caused mitochondrial swelling and loss of mitochondrial membrane potential (39). Our finding of increasing toxicity accompanying zinc supplementation suggests that in tumor cells clioquinol may act by increasing intracellular metal levels, perhaps in key compartments, such as the mitochondria, which has been shown to be susceptible to injury when loaded with metals (40). The alterations of mitochondrial membrane potential may lead to cytochrome *C* release and initiate apoptosis cascade in targeted cells. In line with this hypothesis, we have found that clioquinol induces apoptosis and PARP cleavage in Raji cells. The involvement of NFκB signaling in clioquinol-induced apoptosis needs to be further investigated inasmuch as NFκB activity has been known to be related to apoptosis (35).

Taken together, these studies indicate that metal chelators may act through disparate mechanisms. Metal-binding agents may or may not be able to enter cells (in either a free or bound form), which will play an important role in determining their effects on cells. The ability of a chelator that enters cells to act as an ionophore likely depends on several additional factors. The lipophilicity of clioquinol, its modest affinity for zinc, and its pK_a for deprotonation of the phenolic group (8.07) are likely important determinants of its ability to act as an ionophore and as an effective cytotoxic agent. As with other potential anticancer drugs, careful assessment of their risks and benefits must be undertaken, but transition metal ionophores such as clioquinol seem to be worthy of further exploration as potential anticancer agents.

Acknowledgments

Received 10/5/2004; revised 1/31/2005; accepted 2/4/2005.

The costs of publication of this article were defrayed in part by the payment of page charges. This article must therefore be hereby marked *advertisement* in accordance with 18 U.S.C. Section 1734 solely to indicate this fact.

References

1. Desoize B. Metals and metal compounds in carcinogenesis. In Vivo 2003;17:529–39.
2. Toyokuni S. Iron-induced carcinogenesis: the role of redox regulation. Free Radic Biol Med 1996;20:553–66.
3. Theophanides T, Anastassopoulou J. Copper and carcinogenesis. Crit Rev Oncol Hematol 2002;42:57–64.
4. Brewer GJ. Copper control as an antiangiogenic anticancer therapy: lessons from treating Wilson's disease. Exp Biol Med (Maywood) 2001;226:665–73.
5. Lovejoy DB, Richardson DR. Iron chelators as antineoplastic agents: current developments and promise of the PIH class of chelators. Curr Med Chem 2003;10:1035–49.
6. Pan Q, Kleer CG, van Golen KL, et al. Copper deficiency induced by tetrathiomolybdate suppresses tumor growth and angiogenesis. Cancer Res 2002;62:4854–9.
7. Brewer GJ, Dick RD, Grover DK, et al. Treatment of metastatic cancer with tetrathiomolybdate, an anticopper, antiangiogenic agent: phase I study. Clin Cancer Res 2000;6:1–10.
8. Redman BG, Esper P, Pan Q, et al. Phase II trial of tetrathiomolybdate in patients with advanced kidney cancer. Clin Cancer Res 2003;9:1666–72.

9. Abeysinghe RD, Greene BT, Haynes R, et al. p53-independent apoptosis mediated by tachpyridine, an anti-cancer iron chelator. Carcinogenesis 2001;22:1607–14.

10. Fan L, Iyer J, Zhu S, et al. Inhibition of N-*myc* expression and induction of apoptosis by iron chelation in human neuroblastoma cells. Cancer Res 2001;61:1073–9.

11. Pan Q, Bao LW, Merajver SD. Tetrathiomolybdate inhibits angiogenesis and metastasis through suppression of the NFκB signaling cascade. Mol Cancer Res 2003;1:701–6.

12. Hollingshead R. The dihalogen and trihalogen derivatives. In: Oxine and its derivatives, vol. III. London: Butterworths Scientific Publications; 1956. p. 740.

13. Tsubaki T, Honma Y, Hoshi M. Neurological syndrome associated with clioquinol. Lancet 1971;1:696–7.

14. Meade TW. Subacute myelo-optic neuropathy and clioquinol. An epidemiological case-history for diagnosis. Br J Prev Soc Med 1975;29:157–69.

15. Cherny RA, Atwood CS, Xilinas ME, et al. Treatment with a copper-zinc chelator markedly and rapidly inhibits β-amyloid accumulation in Alzheimer's disease transgenic mice. Neuron 2001;30:665–76.

16. Kaur D, Yantiri F, Rajagopalan S, et al. Genetic or pharmacological iron chelation prevents MPTP-induced neurotoxicity *in vivo*: a novel therapy for Parkinson's disease. Neuron 2003;37:899–909.

17. Regland B, Lehmann W, Abedini I, et al. Treatment of Alzheimer's disease with clioquinol. Dement Geriatr Cogn Disord 2001;12:408–14.

18. Ritchie CW, Bush AI, Mackinnon A, et al. Metal-protein attenuation with iodochlorhydroxyquin (clioquinol) targeting Aβ amyloid deposition and toxicity in Alzheimer disease: a pilot phase 2 clinical trial. Arch Neurol 2003;60:1685–91.

19. Huang P, Feng L, Oldham EA, et al. Superoxide dismutase as a target for the selective killing of cancer cells. Nature 2000;407:390–5.

20. Liu B, Fan Z. The monoclonal antibody 225 activates caspase-8 and induces apoptosis through a tumor necrosis factor receptor family-independent pathway. Oncogene 2001;20:3726–34.

21. Liu B, Fang M, Schmidt M, et al. Induction of apoptosis and activation of the caspase cascade by anti-EGF receptor monoclonal antibodies in DiFi human colon cancer cells do not involve the c-*jun* N-terminal kinase activity. Br J Cancer 2000;82:1991–9.

22. Liu B, Peng D, Lu Y, et al. A novel single amino acid deletion caspase-8 mutant in cancer cells that lost proapoptotic activity. J Biol Chem 2002;277:30159–64.

23. Sun J, Blaskovich MA, Knowles D, et al. Antitumor efficacy of a novel class of non-thiol-containing peptidomimetic inhibitors of farnesyltransferase and geranylgeranyltransferase I: combination therapy with the cytotoxic agents cisplatin, Taxol, and gemcitabine. Cancer Res 1999;59:4919–26.

24. Okado-Matsumoto A, Fridovich I. Assay of superoxide dismutase: cautions relevant to the use of cytochrome *c*, a sulfonated tetrazolium, and cyanide. Anal Biochem 2001;298:337–42.

25. Heikkila RE, Cabbat FS, Cohen G. *In vivo* inhibition of superoxide dismutase in mice by diethyldithiocarbamate. J Biol Chem 1976;251:2182–5.

26. Walsh CT, Sandstead HH, Prasad AS, et al. Zinc: health effects and research priorities for the 1990s. Environ Health Perspect 1994;102 Suppl 2:5–46.

27. Cohen JJ, Duke RC. Glucocorticoid activation of a calcium-dependent endonuclease in thymocyte nuclei leads to cell death. J Immunol 1984;132:38–42.

28. Schrantz N, Auffredou MT, Bourgeade MF, et al. Zinc-mediated regulation of caspases activity: dose-dependent inhibition or activation of caspase-3 in the human Burkitt lymphoma B cells (Ramos). Cell Death Differ 2001;8:152–61.

29. Cho IH, Im JY, Kim D, et al. Protective effects of extracellular glutathione against Zn^{2+}-induced cell death *in vitro* and *in vivo*. J Neurosci Res 2003;74:736–43.

30. Telford WG, Fraker PJ. Preferential induction of apoptosis in mouse CD4+CD8+ α β TCRloCD3 ϵ lo thymocytes by zinc. J Cell Physiol 1995;164:259–70.

31. Kondoh M, Tasaki E, Araragi S, et al. Requirement of caspase and p38MAPK activation in zinc-induced apoptosis in human leukemia HL-60 cells. Eur J Biochem 2002;269:6204–11.

32. Canzoniero LM, Manzerra P, Sheline CT, et al. Membrane-permeant chelators can attenuate Zn^{2+}-induced cortical neuronal death. Neuropharmacology 2003;45:420–8.

33. Kim CH, Kim JH, Moon SJ, et al. Pyrithione, a zinc ionophore, inhibits NF-κB activation. Biochem Biophys Res Commun 1999;259:505–9.

34. Kim CH, Kim JH, Hsu CY, et al. Zinc is required in pyrrolidine dithiocarbamate inhibition of NF-κB activation. FEBS Lett 1999;449:28–32.

35. Pommier Y, Sordet O, Antony S, et al. Apoptosis defects and chemotherapy resistance: molecular interaction maps and networks. Oncogene 2004;23:2934–49.

36. Yassin MS, Ekblom J, Xilinas M, et al. Changes in uptake of vitamin B(12) and trace metals in brains of mice treated with clioquinol. J Neurol Sci 2000;173:40–4.

37. Tanaka H, Tamura Z. Analysis of chinoform binding to human serum albumin by an improved partition equilibrium method. J Pharmacobiodyn 1986;9:1015–22.

38. Stehle G, Sinn H, Wunder A, et al. Plasma protein (albumin) catabolism by the tumor itself-implications for tumor metabolism and the genesis of cachexia. Crit Rev Oncol Hematol 1997;26:77–100.

39. Arbiser JL, Kraeft SK, van Leeuwen R, et al. Clioquinol-zinc chelate: a candidate causative agent of subacute myelo-optic neuropathy. Mol Med 1998;4:665–70.

40. Feng P, Li TL, Guan ZX, et al. Direct effect of zinc on mitochondrial apoptogenesis in prostate cells. Prostate 2002;52:311–8.